Anomalous rainfall and associated atmospheric circulation in the northeast Spanish Mediterranean area and its relationship to sediment fluidization events in a lake

Marianna Soler,[1] Teresa Serra,[1] Jordi Colomer,[1] and Romualdo Romero[2]

Received 15 December 2005; revised 15 June 2006; accepted 31 August 2006; published 9 January 2007.

[1] Changes in the dynamics of sediment transport in a Mediterranean lake (sediment fluidization events) are linked to atmospheric circulations patterns (trough monthly precipitation). In the basins of Lake Banyoles, located in the northeast of Spain, water enters mainly through subterranean springs, and associated fluctuations in the vertical migration of sediment distribution (fluidization events) present episodic behavior as a result of episodic rainfall in the area. The initiation of the fluidization events takes place when the monthly rainfall is ~2.7 times greater than the mean monthly rainfall of the rainiest months in the area, especially in spring (April and May), October, and December. The duration of these events is found to be well correlated with the accumulated rainfall of the preceding 10 months before the process initiation. The rainfall, in turn, is mainly associated with six atmospheric circulation patterns among the 19 fundamental circulations that emerged in an earlier study focused on significant rainfall days in Mediterranean Spain. Among them, accentuated surface lows over the northeast of Spain, general northeasterly winds by low pressure centered to the east of Balearic Islands and short baroclinic waves over the Iberian Peninsula, with easterly flows over the northeastern coast of Spain, are found the most relevant atmospheric circulations that drive heavy rainfall events.

Citation: Soler, M., T. Serra, J. Colomer, and R. Romero (2007), Anomalous rainfall and associated atmospheric circulation in the northeast Spanish Mediterranean area and its relationship to sediment fluidization events in a lake, *Water Resour. Res.*, *43*, W01404, doi:10.1029/2005WR004810.

1. Introduction

[2] Both the spatial and temporal variability of ecological parameters are usually connected to the variability of synoptic atmospheric patterns and certain environmental parameters. *Yarnal* [1993] offers multiple examples of synoptic classifications ranging from subjective manual classifications to outputs from eigenvector-based techniques. Worked examples are used to determine how well these classifications relate to four environmental scenarios in the Pennsylvania area (urban air quality, acid rain, agriculture and fluvial hydrology). *Bonell and Summer* [1992] establish, using S mode principal component analysis and cluster analysis, the main daily precipitation affinity areas for Wales according to surface wind direction. Regional and North Atlantic atmospheric circulation (identified by the North Atlantic Oscillation index sign and strength) have a remarkable impact on aquatic systems, based on effects on water temperature, ice phenology [*Blenckner and Chen*, 2003; *Livingstone*, 1999; *Martin et al.*, 1997; *Omstedt and Chen* 2001], phytoplankton spring blooms [*Blenckner and Chen*, 2003; *Gerten and Adrian*, 2000; *Weyhenmeyer et al.*, 1999], and nitrate, dissolved reactive phosphorous and chlorophyll concentrations [*George et al.*, 2004], although also depending on different thermal lake structures and mixing regimes [*Gerten and Adrian*, 2001].

[3] The Spanish Mediterranean area (Figure 1) possesses a rather complex topography. It is influenced by both Atlantic low-pressure systems (centered to the west and north of the area) and by Mediterranean disturbances (in the eastern part), and it is subject to extreme seasonal contrasts as a result of its latitude (36°–44°N). All these factors yield daily rainfalls of considerable spatial and temporal variability [*Romero et al.*, 1998]. Among the studies related to the Spanish Mediterranean, *Summer et al.* [1995] associate the distribution of significant rainfalls over the island of Mallorca with recognized dominant surface circulation types. Despite the effects of defined atmospheric patterns on hydrology are conceptually recognized and are also apparent through numerous case studies (notably of heavy precipitation events in eastern Spain [see *Doswell et al.*, 1998]), they have been poorly studied for Mediterranean Spain.

[4] In this paper we examine the dynamics of the sediment fluidization in a Mediterranean karstic lake (northeast of Spain), associated with meteorological conditions. The time evolution of sediment fluidizations at the bottom of the

[1]Group of Environmental Physics, Physics Department, University of Girona, Girona, Spain.
[2]Meteorology Group, Physics Department, University of the Balearic Islands, Palma de Mallorca, Spain.

0043-1397/07/2005WR004810

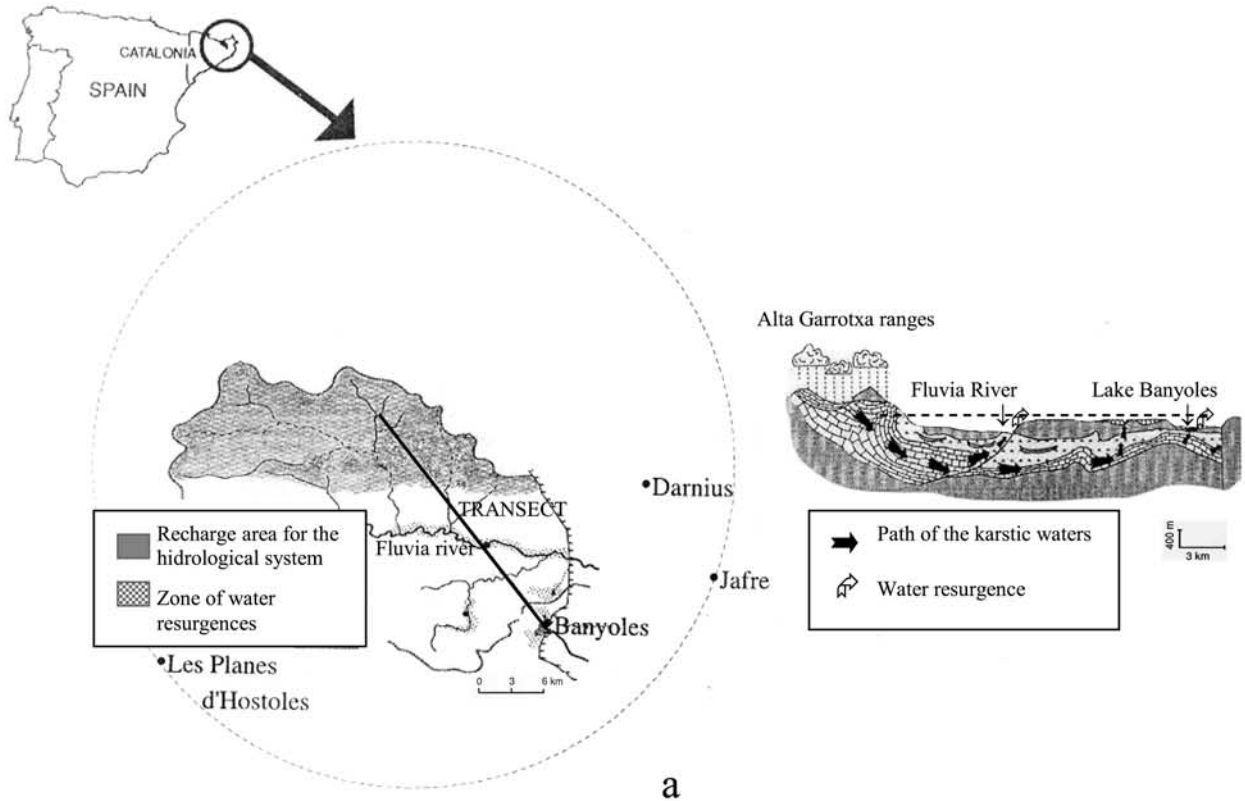
CATALONIA
SPAIN
Alta Garrotxa ranges
Fluvia River
Lake Banyoles
Darnius
TRANSECT
Fluvia river
Jafre
Banyoles
Les Planes
d'Hostoles
Recharge area for the hidrological system
Zone of water resurgences
Path of the karstic waters
Water resurgence
400 m
3 km
0 3 6 km

a

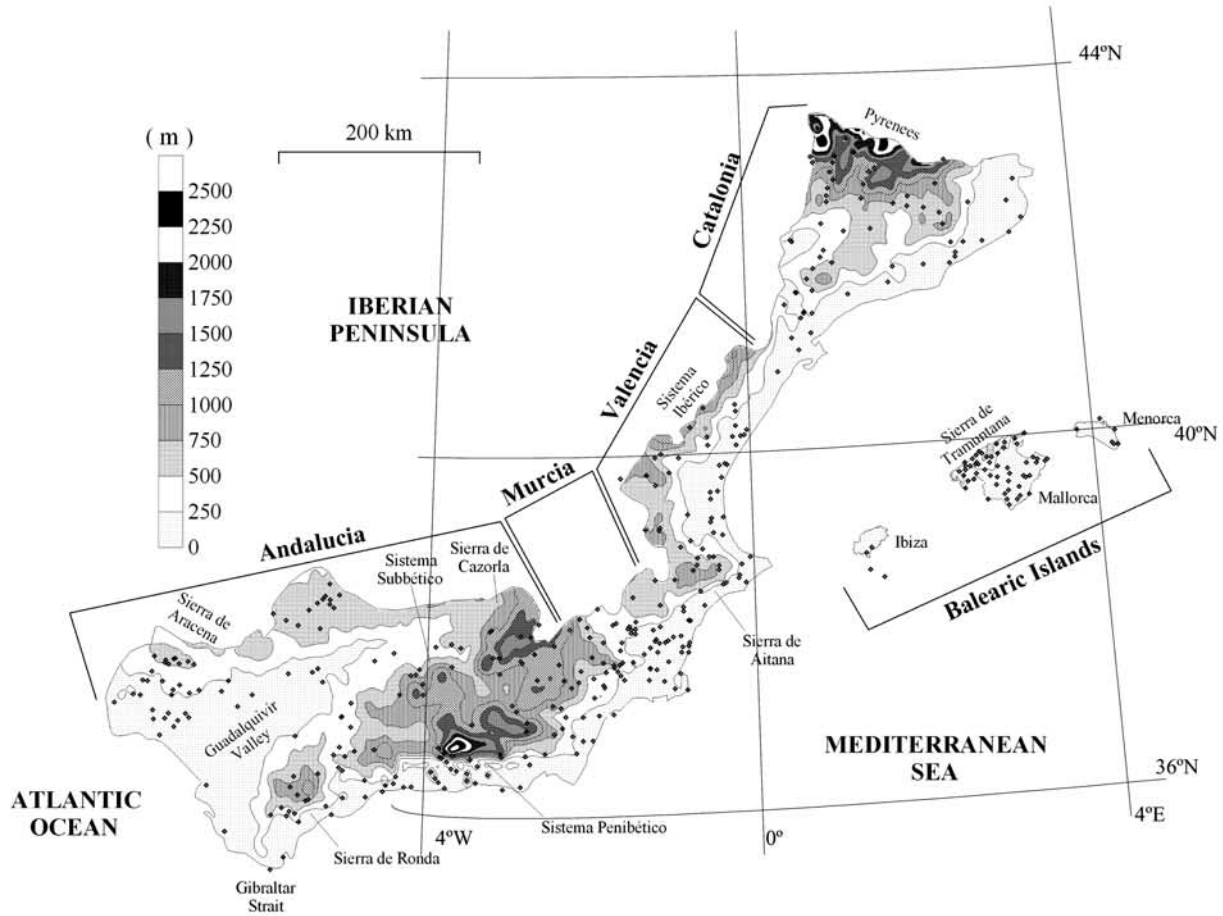
(m)
2500
2250
2000
1750
1500
1250
1000
750
500
250
0
200 km
44ºN
40ºN
36ºN
4ºW
0º
4ºE
Pyrenees
Catalonia
Valencia
Murcia
Andalucia
IBERIAN PENINSULA
Sistema Ibérico
Sistema Subbético
Sierra de Cazorla
Sierra de Aracena
Guadalquivir Valley
Sierra de Aitana
Sierra de Tramuntana
Menorca
Mallorca
Ibiza
Balearic Islands
MEDITERRANEAN SEA
ATLANTIC OCEAN
Sistema Penibético
Sierra de Ronda
Gibraltar Strait

b

Figure 1

basin-lake has been recorded for a total of 22 years (the last 19 years continuously). Records show that the sediment fluidization in basin B2 of the lake develops episodically (episodic fluidization) as a function of the amount of rainfall in the recharge aquifer area (Figure 1a). Sediment fluidizations are of great limnological interest because it is a mechanism that carries particles in suspension from the sediment interface upward into the lake water column, affecting water quality, the fish distribution [*Serra et al.*, 2002] and sedimentary records in the whole lake [*Serra et al.*, 2005]. Therefore it is important to investigate the time series of historical observations of fluidization events in basin B2 in view of linking the relevant synoptic atmospheric circulations and associated rainfall to the water quality and limnology of the lake.

[5] Following this introduction, the paper is organized into various sections. Both the analysis of the meteorological parameters and the observations of sediment fluidizations in basin B2 are described in section 2. In section 3 we present the relationship between the sediment fluidization events and the local rainfall in the recharge area and also compare them with the atmospheric patterns predicted by the atmospheric circulation model. Section 4 summarizes our findings.

2. Data and Analysis

2.1. Study Site

[6] Lake Banyoles (42°07′N, 2°45′E), in the eastern Catalan pre-Pyrenees (Figure 1), is a small multibasin lake (surface area of 1.12 km^2) of mixed tectonic-karstic origin [*Canals et al.*, 1990] composed of six main basins (B1–B6) (Figure 2). One of the most important aspects of the hydrological environment of Lake Banyoles is the fact that basin B1 (the largest basin) supplies around the 85% of the total incoming water by subterranean springs (at approximately 75 m of depth) and the rest is supplied by river flows entering the lake from the southeast. The tectonic constraint of the lake forces the vertical discharge of groundwater flow through the bottom of the basins. In addition, the subterranean springs mix the sediments above them up to a fairly sharp interface known hereafter as the lutocline (Figures 3a and 3b). The sediment in basin B2 usually remains consolidated at the bottom, with the lutocline at a depth of approximately 44 m [*Casamitjana and Roget*, 1993; *Colomer et al.*, 1998]. Episodically, the subterranean springs in B2 supply water to the lake at a rate comparable to B1 (in the order of 0.5 m^3/s). This happens for high-precipitation periods that recharge the aquifer increasing the pressure enough for incoming water to resuspend the confined and consolidated sediment at the bottom of B2 [*Colomer et al.*, 2003].

[7] The relationship between the timing of sediment fluidization events and local monthly rainfall was investigated using daily data from the nearest meteorological stations at Castelló d'Empúries, Jafre, Les Planes d'Hostoles, Banyoles and Darnius. The first three are located ~30 km from the area of aquifer recharge, while Banyoles is ~19 km away and Darnius is at a distance of ~15 km (Figure 1a). The rainfall in the Darnius meteorological station has therefore been chosen as characteristic of the rainfall of the area of aquifer recharge.

2.2. Classification of Daily Atmospheric Circulation Patterns

[8] *Romero et al.* [1999a] derived 19 characteristic atmospheric patterns (APs) responsible for significant rainfall in Mediterranean Spain. Specifically, atmospheric patterns of all days in the period 1984–1993 in which at least 5% of the 410 rain gauge stations shown in Figure 1b registered more than 5 mm (1275 days) were classified into 19 classes (AP) using principal components analysis and cluster analysis (see the details given by *Romero et al.* [1999a]). The classification was based on the flow patterns at 925 and 500 hPa over the region shown in Figure 1b (shown as a shaded square in Figure 10), using the gridded meteorological analyses of the European Centre for Medium-Range Weather Forecasts (ECMWF) as input data. In fact, the synoptic classification was also attempted based on grid analyses of temperature, relative humidity, horizontal wind components and other derived fields as the upslope flow induced by the orography, but the most satisfactory results in terms of the relationship between the resulting atmospheric patterns and certain daily rainfall spatial distributions known for the region [*Romero et al.*, 1999a] were obtained from a combination of the geopotential height fields at 500 and 925 hPa. This is not surprising, since these fields already contain, either explicitly or implicitly, essential information about important dynamic and thermodynamic physical processes behind precipitation generation and distribution: the dynamic forcing for vertical motion by advection of vorticity at upper levels; the presence of cold pools aloft; the sign and intensity of low tropospheric temperature advection; the interaction of low-level flow with the topography; and the moisture content of surface air masses with long paths over the Mediterranean Sea or Atlantic Ocean.

[9] This study requires a long-term seasonal analysis of the AP frequencies and the search for anomalies in their persistence during the fluidization periods. For that purpose, daily atmospheric states during the period January 1970 to August 2002 were matched against the 19 AP types described above (derived from the study of the 1984–1993 period), or as insignificant ("not rainy") situations. Input meteorological data for this long-term classification were taken from the ECMWF ERA-40 reanalysis at 12 Coordinated Universal Time (CUT). This is a long, homogeneous, high-quality database suitable for synoptic-

Figure 1. (a) General location map of Lake Banyoles and schematic representation for the hydrological system in the Lake Banyoles region, including the recharge area for the hydrogeological system and the nearest meteorological stations location. Figure 1a (right) shows the path of karstic water, along the transect marked in the schematic representation (adapted from *Brusi et al.* [1990]). (b) The Spanish Mediterranean area, which comprises the regions of Catalonia, Valencia, Murcia, Andalusia, and Balearic Islands. It includes a smoothed version of its orography, the position of the rain gauge stations (410 in total), and some geographical references mentioned in the text. The two stations adjacent to Ibiza belong to the small island of Formentera, which is not represented.

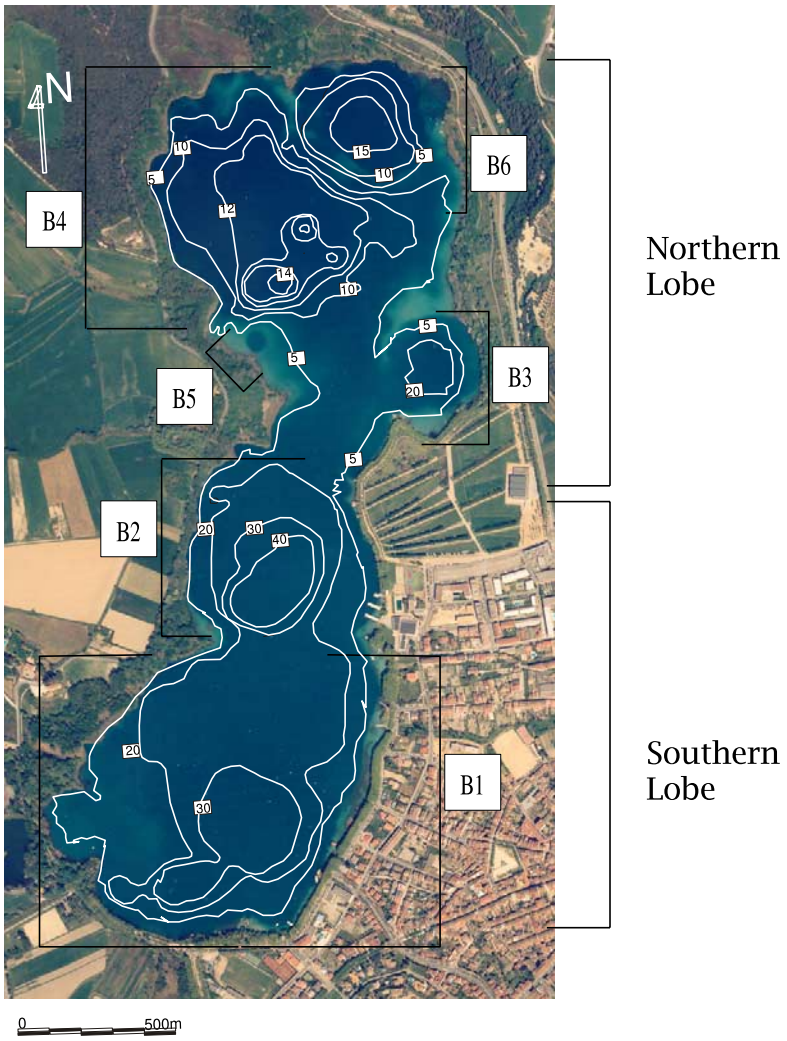

Figure 2. Aerial photograph of Lake Banyoles. The lake is divided into six basins. Basin B1 is located in the southern lobe, basin B2 is in the central lobe, and B3, B4, B5, and B6 are in the northern lobe, some of them clearly seen in the photograph (kindly provided by the Institut Cartogràfic de Catalunya). Also in the plot, contour depths (with characteristic values in meters) are shown.

scale studies like the present one (see http://data.ecmwf.int/data/ for specific information about ERA-40).

[10] Several techniques exist for the matching of individual daily atmospheric patterns to the previously derived 19 'typical' APs. The one chosen classifies the circulation for each ERA-40 day by matching it with the closest observed day within the 1984–1993 ECMWF data set. If the matched day within the ECMWF set was not itself classified within one of the 19 APs then the day is simply considered as a not rainy situation. Matching is performed with a similarity index (d) utilizing the Pearson product-moment correlation coefficients for the combined 925 (r_{925}) and 500 (r_{500}) hPa geopotential height fields:

$$d = \sqrt{(1 - r_{925})^2 + (1 - r_{500})^2} \quad (1)$$

where the correlation coefficient is calculated using the field values at grid points included within the geographic studied area [*Romero et al.*, 1999a]. The closest observed day, is thus defined, as the one presenting the lowest d value. Similar analogue approaches have been used in climate research to good effect [e.g., *Summer et al.*, 2003]. Out of the 11932 days included in the 1970–2002 period, 3953 were classified among the 19 AP classes, thus representing about one third of total days, in close agreement with the observed percentage of significant rainy days in Mediterranean Spain [*Romero et al.*, 1998].

2.3. Historical Observations of Sediment Fluidizations in Basin B2

[11] The fluidization events (F1, F2, etc) were detected by measuring the depth of the lutocline Z_L in basin B2. The lutocline level was well detected by seismic profiles (Figures 3a and 3b), echo sounding profiles (Figure 3c) or continuous temperature profiles of the water column in B2. Temperature profiles showed that the temperature at and below the lutocline in B2 changed from around 17.5°C at the beginning of the fluidization process to 19.1°C in the fluidized state. Those values have been found temporally and spatially (within the lutocline) constant with only slight variations. For all registered values at the lutocline depth an

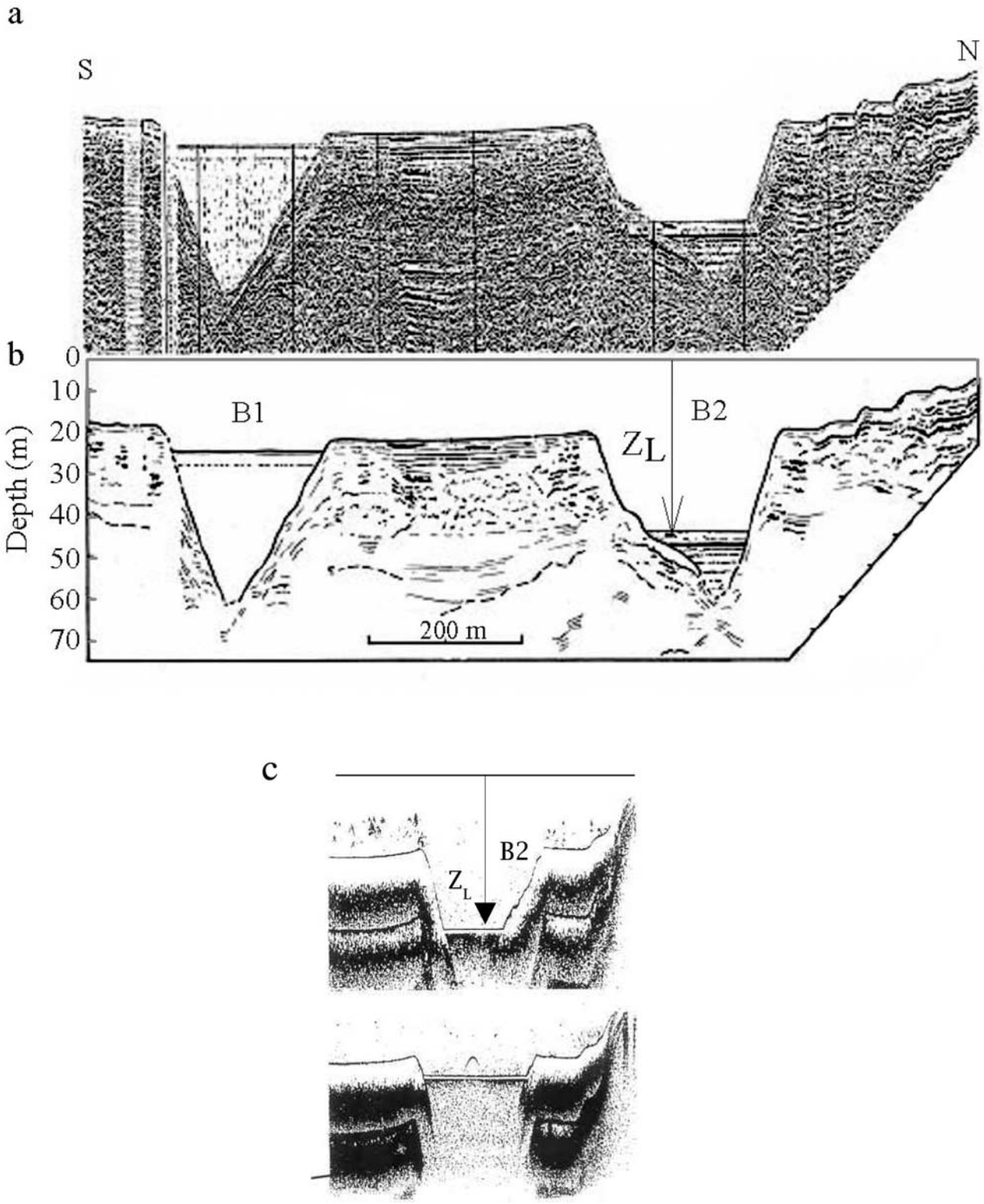

Figure 3. (a) South-north seismic transect and (b) schematic interpretation of the section from B2 to B1 [*Canals et al.*, 1990]. The lutocline is well detected by the seismic profile and is located at a depth Z_L from the surface. (c) Echosounding transect in B2 showing the two states of the sediment bed: (top) nonfluidized and (bottom) fluidized.

inverse temperature gradient of 2°–8°C/m was found. The mean sediment concentration below the lutocline in B2, which appears as a flat line in both the seismic (Figure 3a) and echo sounding profiles (Figure 3c), depends on the state of fluidization, and varied between 100 and 280 g/l. As shown in the south to north seismic transect in Figure 3a, B2 was confined at the bottom (nonfluidized state) with the lutocline located at a depth of 44 m. As shown in Figure 3c,

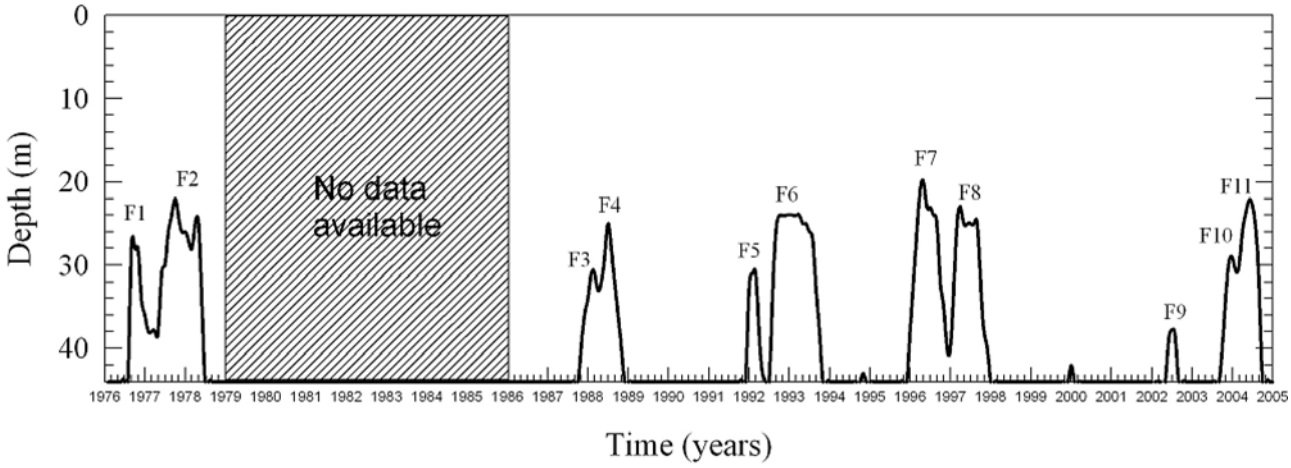

Figure 4. Lutocline depth at B2 (as shown in Figure 3b) during the period 1976–2004, where fluidization events are identified (from F1 to F11). The sampling frequency of the lutocline depth for F1 to F4 was 15 days, while for F5 to F11 it was a week.

the top of the lutocline in the fluidization state has found to migrate upward.

3. Results and Discussion

3.1. Sediment Fluidization Events

[12] In the periods 1976–1978 and 1986–2004, the sediments in B2 presented high temporal variability depending on the fluidization events (Figure 4). Two cases, F1 and F2, were detected in 1976–1978 and nine cases, F3 to F11, in the period of continuous measurements 1986–2004. The strength of a fluidization event was quantified by the maximum vertical migration of the lutocline. On the basis of this the largest migration was detected during the F7 event in 1996–1997, when the lutocline in B2 migrated to a depth of about 20.5 m (24 m, the maximum vertical migration of the lutocline from the historical record). Of remarkable interest is the fact that the major fluidization events may last more than one year, especially because some events are coupled: F1–F2, F3–F4, F5–F6, F7–F8, and F10–F11. This behavior can be explained by taking into account that a second fluidization is more possible in an already fluidized state of the sediments in the basin although the inflow of water is not so high. The fluidizations do not happen each year, they happen episodically, without following any periodic evolution.

3.2. Sediment Fluidization Events Related to Local Rainfall

[13] The mean monthly rainfall in Lake Banyoles (available period: 1986–2004) and in the area of the aquifer recharge (available period: 1987–2004) are shown in Figure 5. On average, monthly rainfalls present marked seasonal variation, with maximum values concentrated in spring and autumn for both meteorological stations. The rainfall in both areas is explained by different circulation patterns: (1) large depressions lying above western Spain, which provide southwesterly-westerly flows and also warm and moistened southerly flows, a pattern essentially linked to the Atlantic dynamics which quasiperiodically influences the Spanish latitudes during the cold season, and (2) southerly-southeasterly onshore flows, cold fronts from the north, and also easterly to northerly flows induced by frequent depressions in the north of the Mediterranean basin, a circulation contributed by Atlantic disturbances circulating at higher latitudes, and also influenced by secondary cyclones generated frequently over the northern part of the Mediterranean basin. The accentuated maximum in October is related to synoptic disturbances that become very effective through the strong interaction between large amounts of water vapor released from the warm Mediterranean and coastal terrain features [*Romero et al.*, 1999b; *Doswell et al.*, 1998]. The relative maximum in December is associated with rainfall related to the passage of cold fronts over the Iberian Peninsula, associated with midlatitude disturbances and mainly affecting the very north of Catalonia, including the area of aquifer recharge.

[14] The local rainfall in the area of aquifer recharge during the months of the initiation of the sediment fluid-

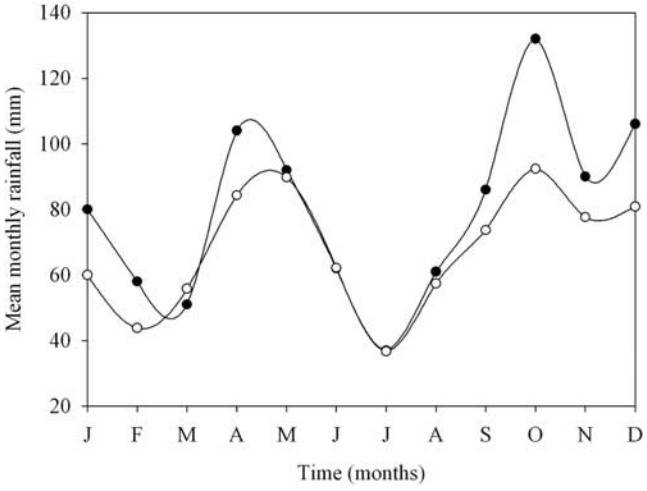

Figure 5. Monthly rainfall in the area of the aquifer recharge (Darnius, solid circles) and in the area of study (Banyoles, open circles). In Darnius, data were available from 1987 to 2004, and in Banyoles, data were available from 1986 to 2004.

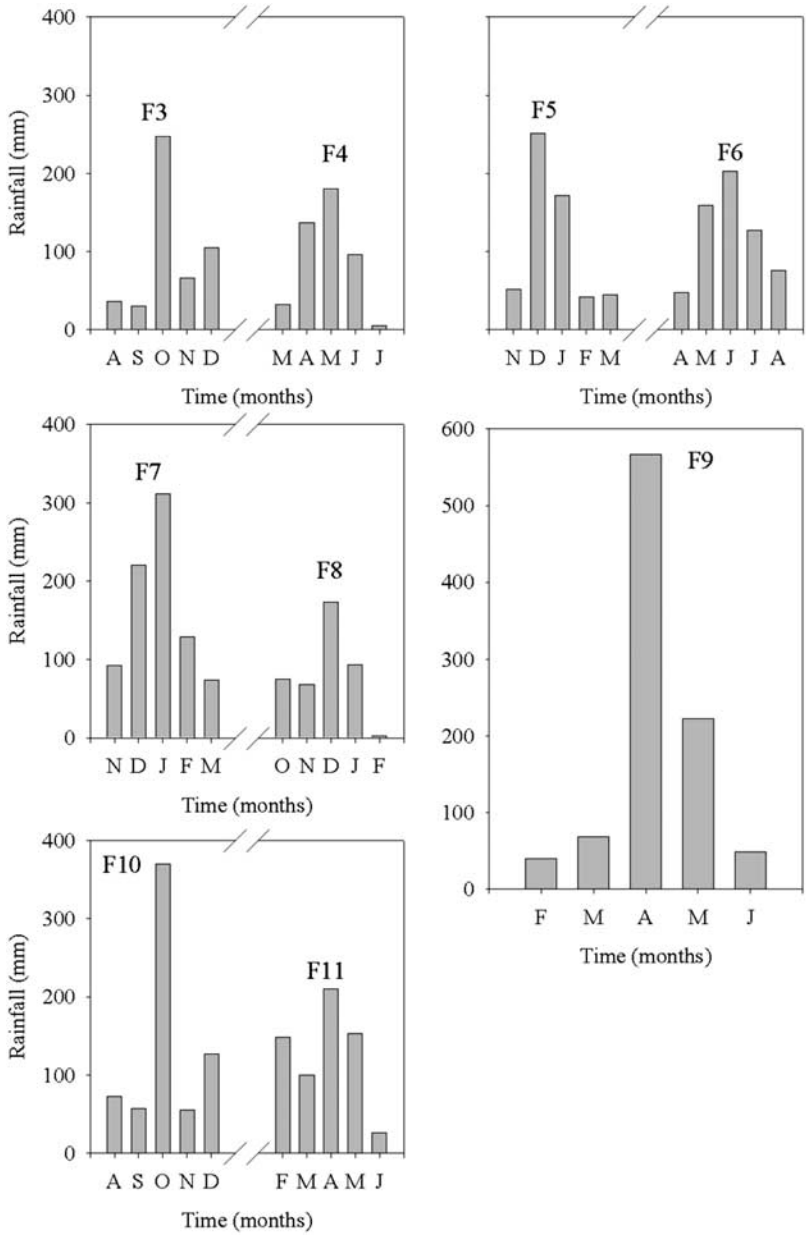

Figure 6. Local monthly rainfall during the fluidization events in the area of aquifer recharge. The central value corresponds to the month of initiation of each fluidization event.

izations in basin B2 of the lake is shown in Figure 6, where the central bar (from the 5 bars in each fluidization) coincides with the month of the initiation of the process. The term initiation of the fluidization refers to the first day on which the vertical displacement of the lutocline was observed (at least $z_L < 42$ m). It should be borne in mind here that the frequency of measurements of z_L is likely to limit the exact estimation of the onset of the fluidization event. On the basis of the vertical water temperature profiles a delay of a week is waited between the day of heavy rainfall and the initiation of lutocline depth vertical migration. Despite this reservation, however, time initiation of each fluidization coincides with the maximum mean monthly rainfall in Figure 6, which was about 250–350 mm (F3, F5, F7 and F10) or larger, 550 mm in the F9 case. For the fluidizations following a previous one (F4, F6, F8 and F11), a monthly local rainfall of about 200 mm is enough to drive the next event in B2. Both Figures 7a and 7b show the rainfall anomaly, which is defined as the difference between the monthly rainfall values and the mean monthly rainfall for the whole period for which data was available, divided by the latter. This illustrates the occurrence of the largest rainfall anomalies during the fluidization events. A value of 200% means that the value of the local monthly rainfall is three times the mean monthly rainfall. The mean anomalies of rainfall in the area of aquifer recharge and in Lake Banyoles, for the months of the initiation of the fluidization events, are 167 and 151 %, respectively. Then, the local monthly rainfalls are 2.67 and 2.51 times the mean monthly rainfall, respectively.

[15] It is worth noting that the extent and duration of a fluidization event not only depends on the local monthly

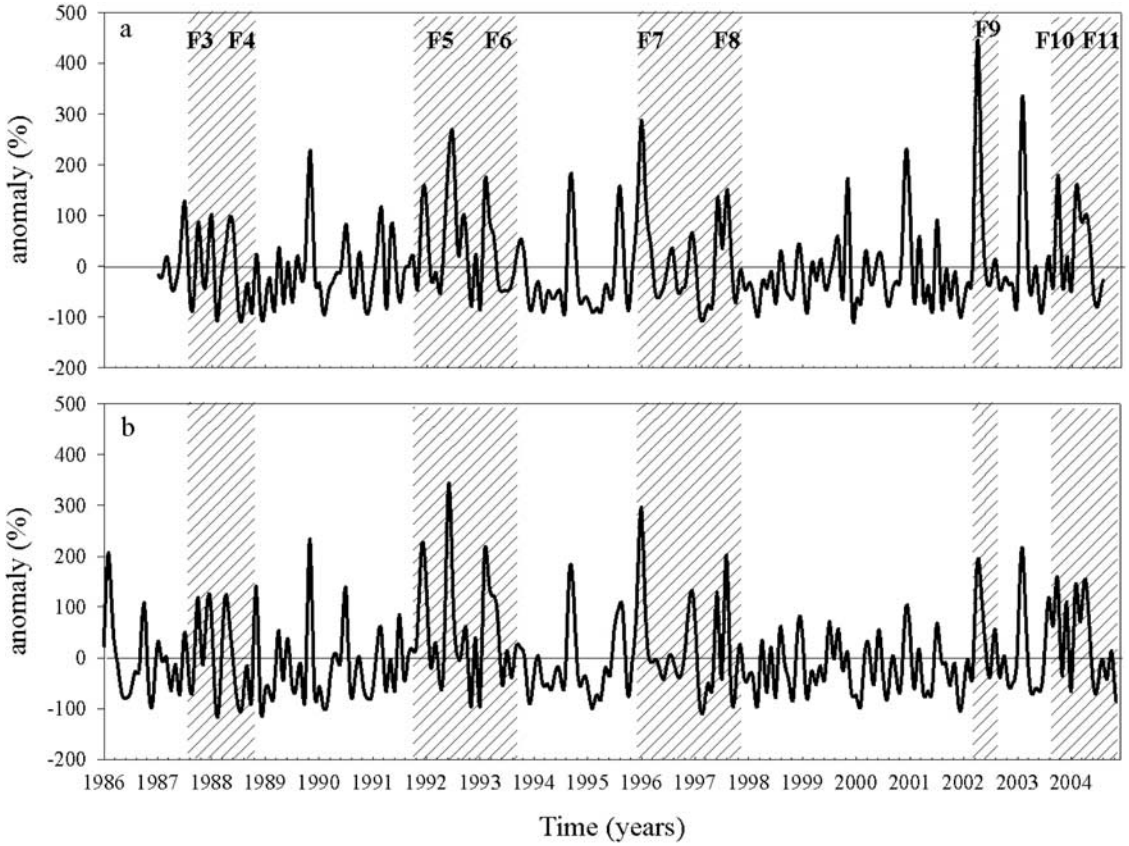

Figure 7. Calculated monthly rainfall anomaly (a) in the area of aquifer recharge (Darnius) and (b) in the area of study (Banyoles).

rainfall of a particular month but on the cumulative monthly rainfall in the months preceding and after the initiation of the process. Fluidization F9 presents an extreme behavior, in that the maximum local monthly precipitation value ever recorded in the area of aquifer recharge (April 2002) drove this fluidization, although with a weak vertical extent and duration, of about 6 m and 4 months, respectively (Figure 4). This fluidization was preceded by a very dry period on the whole, and therefore the sediment could not be maintained in suspension and lutocline migrated down. In contrast, F6 lasted for about 16 months (June 1992 to October 1993) as a result of large sustained precipitation in the area of aquifer recharge. On the basis of this interpretation, another variable comes into question as a possibly useful empirical determinant of the extent of a fluidization event: the accumulated monthly rainfall in the months preceding the event. Thus we can make the assumption that the extent and duration of a fluidization event is associated with monthly rainfall accumulated over some fixed period of time; i.e., that the vertical migration of the lutocline is correlated with the monthly anomalies of local rainfall in the area of aquifer recharge, $P_{J,N}$, defined in discrete form as

$$P_{J,N} = \frac{1}{N} \sum_{j=J-N+1}^{j=J} P_{j,N} \qquad (2)$$

where the location parameter J is the month of the year on which the fluidization process begins, the integrating parameter N is the number of preceding months over which the sum is performed, and $P_{j,N}$ is the monthly rainfall in month j. The best linear relationship between the vertical depth of the lutocline and $P_{J,N}$ (same number of data pairs) is then obtained by finding the values of N that maximize r^2, the proportion of variance explained [*Livingstone*, 1997, 1999]. Values of r^2 were computed at monthly intervals of $3 < N \leq 12$, which included seasonal and annual accumulated rainfall. The maximum explained variance (r^2 = 50.6 %) was obtained with the monthly rainfall accumulated for the previous 10 months (Figure 8). The mean duration of all fluidization events is 10.1 months, which is also in accordance with the mentioned relationship. The result reflects the fact that the tendency in the accumulated rainfall during the previous 10 months determines whether the fluidization will happen or not. In cases where the bed is already fluidized, the rainfall behavior for the previous 10 months will determine its evolution.

[16] The maximum vertical displacement of the lutocline was about 24–22 m, which is limited by the fact that vertical velocity of incoming water diminishes from the inflow at the basin B2 entry (at 85 m of depth) up to the lutocline depth (because of increasing transversal area). At this depth the downward settling vertical velocity of the sediment suspension equals the upward vertical velocity of water [*Colomer et al.*, 2001]. Another factor that limits the maximum excursion of lutocline is the fact that the sediment suspension flowed out the basin because at the south of basin B2 the depth is about 20–22 m; this process would

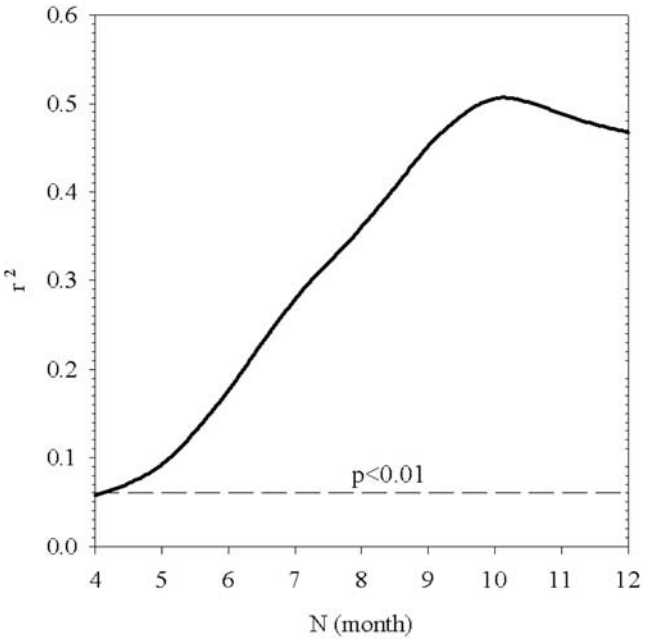

Figure 8. Coefficient of determination (r^2) between the vertical depth of the lutocline and the accumulated rainfall in the area of study on accumulating month N. Significance level ($P < 0.01$) is shown as horizontal dashed line.

only take place during the major fluidization events F6, F7, F8 and F11. Finally, for the coupled fluidizations, the input of water in the aquifer increased its pressure and, as a result, the water entering into an already fluidized bed could produce a secondary migration of the lutocline that reached shallower depths, as in the F3–F4 and F10–F11 cases.

[17] Out of the 11 fluidization processes, 6 took place in the expected seasons of maximum rainfall: spring and autumn (as shown in Figure 5), 4 cases: F1, F5, F7 and F8 took place in winter, as a direct result of the local monthly rainfall of December, and only F6 initiated a fluidization in the warm season of summer (June 1992). In the period 1986–2004, the sediment bed in B2 remained in suspension during a period of 39.9% of the whole historical record.

3.3. Sediment Fluidization Events Related to Atmospheric Patterns

[18] The classification of daily atmospheric circulations for the period 1970–2002 described in the previous section allowed the daily rainfalls in the area of study to be associated with certain of the 19 APs. The APs may be compared with each other in terms of both 500 and 925 hPa circulation dissimilarities within the considered geographical window. In some cases, the structures at 500 hPa, which are smoother, are relatively similar but the surface circulations exhibit substantial differences. In other cases, both levels show very similar aspects in some areas, but in other areas important differences in the position, orientation, size or depth of the disturbance appear [*Romero et al.*, 1999b]. In this section, though, only the most frequent atmospheric patterns during the months of onset of the fluidization events (comprising a total of 525 days) are studied in detail. Here we consider an atmospheric pattern to be relevant if its frequency is larger than 5%. Accordingly, the atmospheric patterns AP3, AP4, AP8, AP9, AP14 and AP19 were identified as the most frequent at the time of initiation of the fluidization events (Figure 9): AP8 (18%), AP19 (12%), AP14 (11%), AP3 (9%), AP4 (7%) and AP9 (7%) account for a total of 64% of all days. These atmospheric patterns are shown in Figure 10 and will be later described in detail. A chi-square test has been carried out to elucidate the significance of these atmospheric patterns during the fluidization events in front of atmospheric patterns during the whole period (1970–2002). Significant differences ($p < 0.05$) were found for the analysis test. Therefore statistics confirm that the fluidization events are related to definite atmospheric patterns in the area of study.

[19] Also, for the whole 1970–2002 data set, the monthly incidence of each AP (from AP1 to AP19) with respect to the total number of days presenting any AP is quantified by introducing the so-called month-frequency ratio ($AP_{ijmonth\text{-}frequency}$). For the calculation it has been used the data for the whole period (Figure 11) without considering the non rainy days (with AP = 0), as follows:

$$AP_{ijmonth-frequency} = \frac{N(AP_{ij})}{\sum_{i=1}^{i=19} N(AP_{ij})} \quad (3)$$

where $N(AP_{ij})$ is the number of days with an AP in the month j. This index is useful to assess the monthly AP climatology in the Spanish Mediterranean area for the 33-year period, i.e., to determine to which degree each AP is expected in any given month on rainy days.

[20] Pattern AP3 (Figure 10a) is characterized by deep depressions centered to the northwest of the Iberian Peninsula. At upper levels, the nearly meridionally oriented transverse axis implies a general southwesterly flux and advection of positive vorticity over the whole of the Mediterranean region of Spain. In the eastern part of the region, there is warm and humid advection from the south-southeast, favoring rainfall development over the exposed

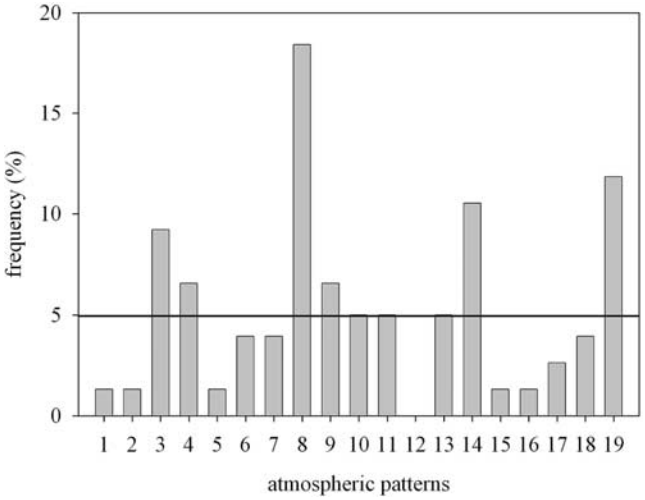

Figure 9. Percentage frequency of each atmospheric pattern during the period of initiation of the fluidization events in basin 2, Lake Banyoles (1976–2004).

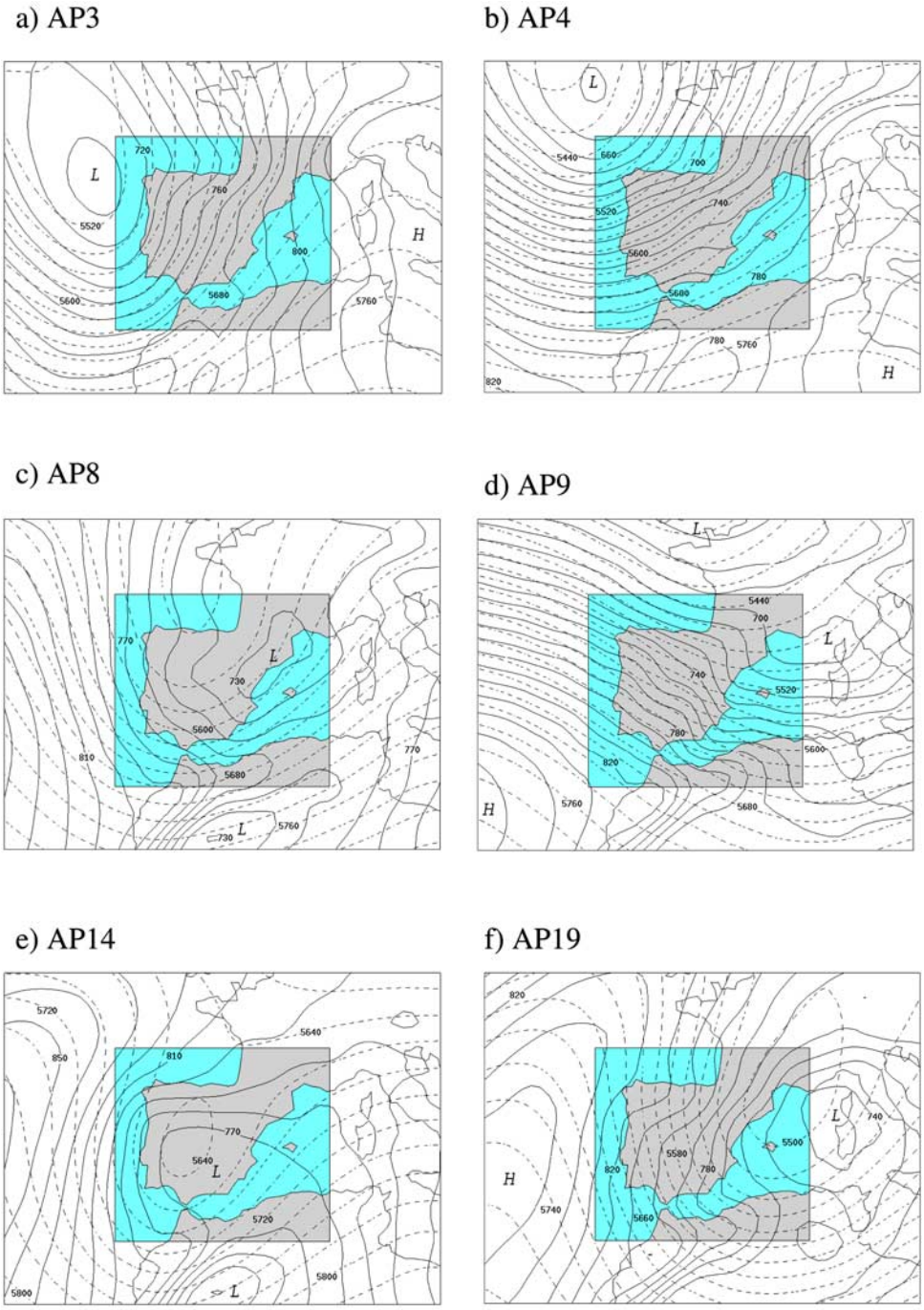

Figure 10. Composites of the six most frequent APs during fluidization events. The solid lines represent the geopotential height field at 925 hPa (contour interval, 10 m), and the dashed lines represent it at 500 hPa (contour interval, 20 m). The interior rectangle represents the geographical window used for the pattern classification.

areas of eastern Spain, including Catalonia. Pattern AP3, comparatively frequent during fluidization episodes (9%, Figure 9), exhibits its maximum occurrence during autumn, especially in October (10.6%) and November (10.8%). These values are above the values during spring and winter (Figure 11). AP3 was found to be mainly developed in fluidizations F3 and F5.

[21] Circulation AP4 (Figure 10b) represents southwesterly flows at all levels associated with low-pressure systems to the northwest of Spain. Characteristically, the geopotential fields indicate the presence of weak cold fronts moving into the Iberian Peninsula from the west. Apart from the Atlantic rainfall patterns that affect the west of Catalonia, rainfall in the area of study is also favored. This circulation presents almost equal month-frequencies in August, October, and December (Figure 11), and seasonally it presents the highest frequency in winter and autumn. It showed high occurrence in fluidization F1, F7 and F8.

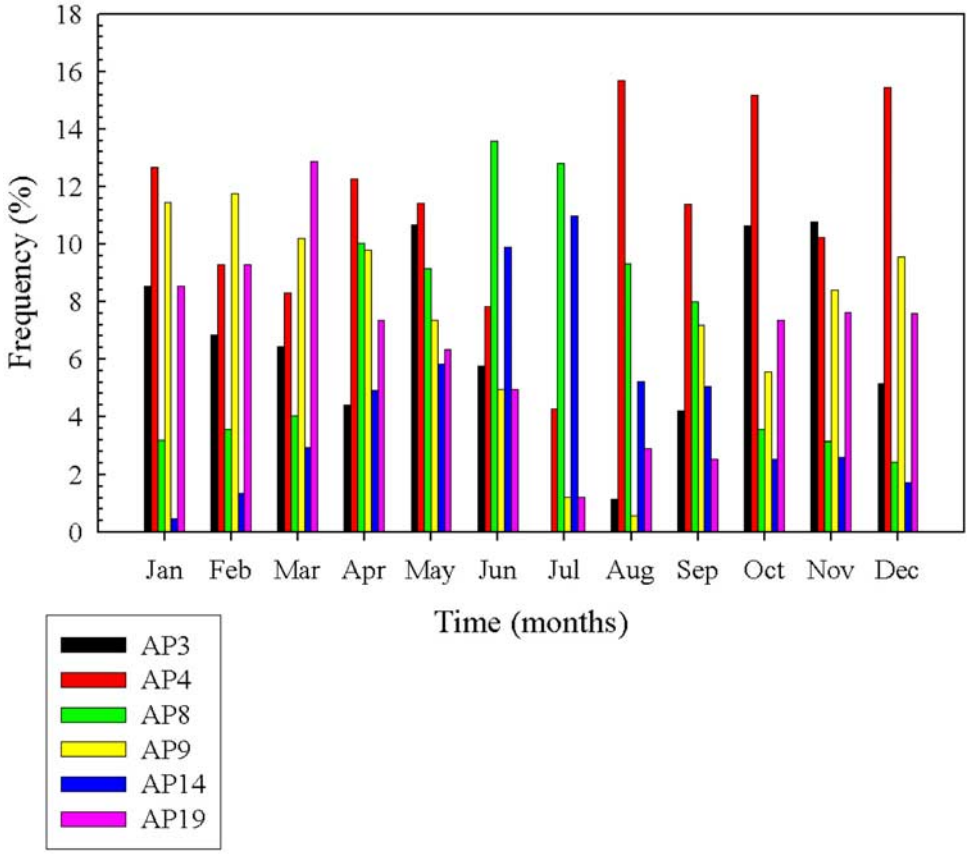

Figure 11. Month-frequency (see text) for the six most frequent APs during fluidization events. The shaded rectangles represent the geographical windows used for the pattern classification.

[22] The most persistent circulation during the onset of the fluidization events, AP8 (Figure 10c), presents occasions when short baroclinic waves occur over the Iberian Peninsula. The general circulation is characterized by deep troughs in the westerlies at upper levels lying over western Spain, but no appreciable tilting. At the surface, the northwesterly winds are associated with the passage of cold fronts. Rainfalls in Catalonia are largely activated by this pattern since that area is affected by maximum positive vorticity advection at 500 hPa. In addition, moisture from the Mediterranean is available ahead of the cold front. AP8 tends to appear in summer (June and July), followed in frequency by spring (April and May). It developed mainly during fluidizations F6, F9 and episodically in F5 (December 1991). However, this atmospheric pattern is not considered frequent for that month of the year (Figure 11).

[23] The AP9 (Figure 10d) basically represents west to northwesterly winds at all levels following the passage of cold fronts from the Atlantic to the Mediterranean. This appears to be an ideal situation for the development of orographically enhanced rainfalls in the South Mediterranean. The northeastern regions (Catalonia and the Balearic Islands) are close to the cold front and this is reflected in the typical rainfalls of winter and spring, where it presents large month-frequencies (Figure 11). It showed high occurrence in fluidization F2.

[24] Pattern AP14 (Figure 10e) is characterized at 500 hPa by an accentuated trough with a positively tilted axis which is restricted to the central part of the Iberian Peninsula. The area with maximum advection of vorticity is the southeast and east, which also benefits from rainfall generated by the warm and humid Mediterranean flows induced by the surface pressure distribution. Rainfalls in the interior of Andalusia (see Figure 1b), which is the nearest zone to the centre of the disturbance and receives favorable northwesterly surface winds, are also produced. Rainfall also occurs in the exposed Pyrenees. This circulation pattern exhibits its maximum month-frequency in the months of summer and spring (Figure 11), and the 925 hPa geopotential fields indicates relatively low pressure areas over the Iberian and African plateau, a signature of warm season thermal lows. This circulation was episodically present in fluidizations F2, F4 and F9. It should be remarked that in April 2002, in the area of aquifer recharge, it rained 324.5 mm (the largest value registered for the whole period of analysis), and it has been associated to the short F9 event (Figure 4).

[25] Finally, cluster AP19 (Figure 10f) comprises 500 hPa lows over the Gulf of Lyon with associated low-level cyclone to the east of the Balearic Islands, which may drive strong rainfall in the northeast of Catalonia. This circulation pattern exhibits high frequency during fluidization periods (Figure 9) and is more frequent in the months of spring and winter (Figure 11) than in autumn. It showed high occurrence in fluidizations F2 and F5.

[26] Also, we can define the $AP_{ij\text{-}frequency}$ (complementary to the previous month-frequency). It is defined as the ratio between the number of days in a month with one AP to the

Table 1. AP Frequencies for All APs, Grouped by Seasons

AP	Winter	Spring	Summer	Autumn
1	42.5	27.5	5.2	24.8
2	53.4	19.9	1.7	25.0
3	29.5	30.5	6.2	33.8
4	32.8	27.8	11.7	27.8
5	27.8	28.6	10.5	33.1
6	26.9	32.5	10.8	29.7
7	23.8	31.0	19.7	25.5
8	14.8	37.9	28.8	18.5
9	40.1	33.2	4.7	22.0
10	39.5	20.9	2.3	37.2
11	3.3	24.2	60.1	12.4
12	32.4	29.7	2.7	35.1
13	40.8	22.4	4.6	32.2
14	9.3	35.8	33.8	21.2
15	24.5	32.7	20.4	22.4
16	11.9	28.6	34.6	24.9
17	34.2	20.8	14.2	30.8
18	31.3	31.9	12.4	24.5
19	35.0	36.0	6.6	22.4

number of total days with the same AP during the whole period studied (12 months), as follows:

$$AP_{ij-frequency} = \frac{N(AP_{ij})}{\sum_{j=1}^{j=12} N(AP_{ij})} \quad (4)$$

where $N(AP_{ij})$ is the number of days with an AP, for i = 1 to i = 19, in a month. This frequency gives information about the most relevant months for each AP; this data is summarized in Table 1 where the $AP_{ij\text{-frequency}}$ for each season (winter, spring, summer and autumn) for the whole period of analysis (1970–2002) are presented. The Atlantic type circulations AP3 and AP4 (associated with fluidizations F1, F3 and F7) show similar frequencies in winter, spring and autumn; and AP9 shows an accentuated maximum in winter followed by spring. The Mediterranean type circulation AP19 showed its maximum in spring and winter, while AP8 and AP14 presented maximum values in spring and summer (minimum in winter). A series of chi-square test, with the data in Table 1, as the observed frequencies and an equal breakdown (25% in each season) as the expected frequencies, were carried out. Significant results ($p < 0.05$) were found for all cases but AP7 and AP15.

[27] When the incidence of the atmospheric circulation patterns during fluidization events is compared against their total incidence, the results can be summarized by the fact that the derived APs for all days belonging to the months of initiation of the fluidization events (a total of 525 days) exhibit large positive anomalies, 84.2% and 83.1%, respectively, compared to the monthly frequency (equation (3)) and AP frequency (equation (4)) derived for the whole set of days. Finally, even though these statistics give information on AP climatology, the type of rainfall episodes associated with the fluidization events under the responsible circulation patterns is not immediately clear. This is briefly discussed in next section.

3.4. Atmospheric Patterns and Torrential Rainfalls

[28] Two types of rainfall episodes are found to act as precursors of fluidizations: (1) moderate to heavy rainfalls occurring in a few days, possibly with torrential character on some days (i.e., greater than 50 mm in 24 h), as in fluidizations F3, F5, F6, F7, F9, F10 and F11, and (2) light to moderate rainfall, but extending (intermittently) over a long enough period (months), as in F4 and F8. A total of 36 torrential rainfalls measured in the period of sediment fluidizations were associated with the most frequent atmospheric patterns AP3, AP4, AP8, AP9, AP14 and AP19. As seen in Figure 12, the six atmospheric patterns present a total of 61.1% of the total number of days with torrential rainfalls. It is noteworthy that AP13, although not very frequent during the fluidization episodes (recall Figure 9), explains a significant fraction of the torrential rainfall registered during the fluidizations (Figure 12). It seems then that AP13 strongly contributed to the rain in the area of study during very few days. This circulation (not shown) represents the presence of large and intense cutoff cyclones over the southern part of the domain, above the Strait of Gibraltar (Figure 1). The associated surface circulation imposes a general easterly regime over the domain, with a continuous supply of moisture toward the Mediterranean coast. Considering all of Mediterranean Spain, AP13 is the atmospheric circulation pattern with the highest propensity toward heavy rain (as much as 38% of AP13 days are torrential). In contrast, the more frequent AP9 pattern for the fluidization phenomenology (Figure 9) exhibits a very low propensity toward heavy rainfalls, both in the study zone (Figure 12) and for the bulk of Mediterranean Spain (less than 4% of AP9 days are torrential somewhere in the area).

[29] Previous studies by *Romero et al.* [1999a] associated torrential rainfall in Mediterranean Spain with atmospheric circulation; they found that in relation to the total rainy days, torrential days have an incidence under situations AP3 and AP14 exceeding 20%, mainly over western Andalusia and eastern Spain, respectively, rather than in the study zone. They also found a certain incidence of torrential rainfall toward the study zone for atmospheric patterns AP13 and AP19, which appears to be consistent with the results shown in Figure 12. All these circulations are characterized in the middle troposphere by closed cyclonic circulations or very accentuated shortwave troughs extending toward the south of the domain. At low levels, they exhibit a significant level of warm advection toward some areas of Mediterranean Spain, particularly Catalonia, except AP19 which is characterized by northerly flows and thus cold advection. Previous studies [*Romero et al.*, 1998, 1999b] also found the preference of heavy precipitations in coastal areas and interior mountainous zones, which is the case in the area of study because of its proximity to the Pyrenees ranges. This scenario has a specific importance in the autumn season, as synoptic disturbances become very effective through the strong interaction between large amounts of water vapor released from the warm Mediterranean and coastal terrain.

3.5. Sediment Fluidizations and Water Quality

[30] On the basis of the above timing of initiation and duration of fluidizations a major limnological implication comes into question: fluidizations F1, F3, F5, F7, F8, F10 and F11 in Lake Banyoles either initiated or initially developed when the water column of the lake was mixed; the mixing period of the lake was established between the

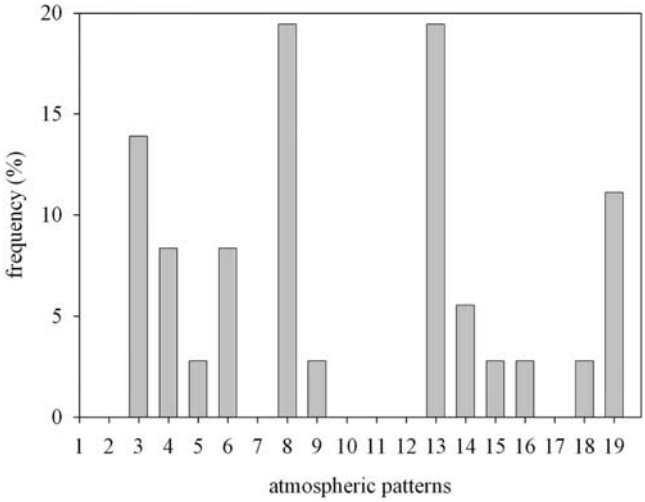

Figure 12. Percentage frequency of torrential days during the time of initiation of the fluidization events as a function of atmospheric pattern (1976–2004).

end of October and mid-April and the rest of time the water column of the lake was stratified. In addition, *Colomer et al.* [2001] found the lutocline to be warmer (because water entry at the bottom of the basins is 19.1°C, as mentioned previously) than the water above the lutocline. The difference in temperature between the suspension zone and the water above induces the development of a turbulent convective plume above the lutocline. As a major characteristic of convection from an isolated source, the plume entrains particles from the lutocline and carries upward a suspension of clay and silt particles with particle volume concentrations of $\sim$5–10 μL L^{-1}. Because of the temperature inversion at the lutocline, the plume is positively buoyant. As a result, it develops upward and in the absence of a thermal stratification background or in the presence of a weak one (as it is in the mixed lake period) it is expected to reach the surface waters after which it spreads laterally, with the consequent change of water quality in terms of an increase of the suspended particle concentration. It can be expected, then, that the suspended particles change the clarity of the water, which might imply a habitat constraint for fishes as limiting their feeding opportunities and other visual activities [*Moyle and Cech*, 1996; *Mathews*, 1998; *Garcia-Berthou*, 1999; *Serra et al.*, 2002]. Also, a stronger effect than limiting the visibility for fish would be the attenuation of light caused by an increase of particle volume concentrations of suspended sediment as high as $\sim$8–29 times the usual values [*Colomer et al.*, 2002] thus limiting photosynthetic radiation available for phytoplankton, affecting the biomass and thus higher trophic levels.

4. Conclusions

[31] This study presents data on sediment fluidization events in Lake Banyoles and their relationship with accumulated rainfall in the recharge area. The characteristic rainfall described by means of atmospheric patterns over the studied area have been analyzed. Among the 19 circulation atmospheric patterns, the Atlantic types: AP3, AP4 and AP9, and the Mediterranean types: AP8, AP14 and AP19, have been found to be responsible for the large or torrential rainfall over the recharged area and associated to the sediment fluidization events in the lake. AP13 has also been found to explain a significant fraction of the torrential rainfall. Out of the 11 fluidization processes, 6 took place in the expected seasons of maximum rainfall: spring and autumn, 4 cases (F1, F5, F7 and F8) took place in winter, as a direct result of the local monthly rainfall of December, and only F6 initiated a fluidization in the warm summer season. Two types of rainfall episodes are found to act as precursors of fluidizations: (1) moderate to heavy rainfalls occurring in a few days, possibly with torrential character on some days, as in fluidizations F3, F5, F6, F7, F9, F10 and F11, and (2) light to moderate rainfall, but extending (intermittently) over a long enough period (months), as in F4 and F8.

[32] It has been found that the lutocline migrated a maximum distance of about 24–22 m while for one case, F9, the lutocline migration was shorter than in the other cases, probably due to the fact that fluidization occurred after a large dry period which could have produced a decrease in the water level of the aquifer. The large excursion observed in the major set of fluidization (F6, F7, F8 and F11) is limited by the fact that vertical velocity of incoming water diminishes from the inflow at the basin entry (at 85 m of depth) up to the lutocline depth. In all probability, the maximum excursion of lutocline is, in fact, limited by the bathymetry of the basin surround which made the sediment suspension flow out the basin because at the south of basin B2 the depth is about 20–22 m. Finally, for the coupled fluidizations, the input of water in the aquifer increased its pressure and, as a result, the water entering into an already fluidized bed could produce a secondary migration of the lutocline that reached upper distances, i.e., less depth if measuring from the water surface, as in the F3–F4 and F10–F11 cases. All in all, the major fluidization events described herein produce large charges in the hypolimnetic waters of the Lake Banyoles because of the heat associated with the incoming warm waters, which, in turn, affect the whole column structure of the lake, especially in the mixing period, and also a substantial increase of suspended sediment that produced changes in the water quality of the lake.

[33] **Acknowledgments.** Precipitation data were provided by the "Instituto Nacional de Meteorologia," stations of Jafre, Les Planes d'Hostoles, and Castelló d'Empúries. We also would like to thank the people in charge of the meteorological stations of Darnius and Banyoles. We thank Anna Vila for helping in the statistics process of the data and Xavier Casamitjana and Elena Roget for providing valuable data on migration of sediments in the lake Banyoles. The authors are also grateful to Captain Joan Corominas for the outstanding help and support in the field campaign. Thanks go also to Josep Pasqual (meteorological station of L'Estartit) for providing some of the temperature data in basin B2. The funds for this research were provided by the "Ministerio de Ciencia y Tecnología" (MCYT) projects REN2001-2239/HID and CGL 2004-02027.

References

Blenckner, T., and D. L. Chen (2003), Comparison of the impact of regional and North Atlantic atmospheric circulation on an aquatic ecosystem, *Clim. Res.*, *23*, 131–136.

Bonell, M., and G. Summer (1992), Atmospheric circulation and daily precipitation in Wales, *Theor. Appl. Climatol.*, *46*, 3–25.

Brusi, D., J. Bach, and M. Sanz (1990), *Itinerari Geòlogic de Banyoles* (in Catalan), Eumo, Barcelona, Spain.

Canals, M., H. Got, R. Julia, and J. Serra (1990), Solution-collapse depressions and suspensates in the limnocrenic lake of Banyoles (NE Spain), *Earth Surf. Processes Landforms*, *15*, 243–254.

Casamitjana, X., and E. Roget (1993), Resuspension of sediment by focused groundwater in Lake Banyoles, *Limnol. Oceanogr.*, *38*, 643–656.

Colomer, J., J. A. Ross, and X. Casamitjana (1998), Sediment entrainment in karst basins, *Aquat. Sci.*, *60*, 338–358.

Colomer, J., T. Serra, J. Piera, E. Roget, and X. Casamitjana (2001), Observations of a hydrothermal plume in a karstic lake, *Limnol. Oceanogr.*, *46*, 197–203.

Colomer, J., T. Serra, M. Soler, and X. Casamitjana (2002), Sediment fluidization events in a lake caused by large monthly rainfalls, *Geophys. Res. Lett.*, *29*(8), 1260, doi:10.1029/2001GL014299.

Colomer, J., T. Serra, M. Soler, and X. Casamitjana (2003), Hydrothermal plumes trapped by thermal stratification, *Geophys. Res. Lett.*, *30*(21), 2092, doi:10.1029/2003GL018131.

Doswell, C. A. III, C. Ramis, R. Romero, and S. Alonso (1998), A diagnostic study of three heavy precipitation episodes in the western Mediterranean regions, *Weather Forecasting*, *13*, 102–124.

Garcia-Berthou, E. (1999), Spatial heterogeneity in roach *Rutilus rutilis* diet among contrasting basins within a lake, *Arch. Hydrobiol.*, *1456*, 239–256.

George, D. G., S. C. Maberly, and D. P. Hewitt (2004), The influence of the North Atlantic Oscillation on the physical, chemical and biological characteristics of four lakes in the English Lake District, *Freshwater Biol.*, *49*, 760–774.

Gerten, D., and R. Adrian (2000), Climate-driven changes in spring plankton dynamics and the sensitivity of shallow polymictic lakes to the North Atlantic Oscillation, *Limnol. Oceanogr.*, *45*, 1058–1066.

Gerten, D., and R. Adrian (2001), Differences in the persistency of the North Atlantic Oscillation signal among lakes, *Limnol. Oceanogr.*, *46*, 448–455.

Livingstone, D. M. (1997), Break-up dates of Alpine lakes as proxy data for local and regional mean surface air temperatures, *Clim. Change*, *37*, 407–439.

Livingstone, D. M. (1999), Ice break-up on southern Lake Baikal and its relationship to local and regional air temperatures in Siberia and to North Atlantic Oscillation, *Limnol. Oceanogr.*, *44*, 1486–1497.

Martin, E., B. Timal, and E. Brun (1997), Downscaling of general circulation model outputs: Simulations of the snow climatology of the French Alps and sensitivity to climate change, *Clim. Dyn.*, *13*, 45–56.

Mathews, W. J. (1998), *Patterns in Freshwater Fish Ecology*, CRC Press, Boca Raton, Fla.

Moyle, P. B., and J. J. Cech, Jr. (1996), *Fishes: An Introduction to Ichthyology*, Prentice-Hall, Upper Saddle River, N. J.

Omstedt, A., and D. L. Chen (2001), Influence of atmospheric circulation on the maximum ice extent in the Baltic Sea, *J. Geophys. Res.*, *106*, 4493–4500.

Romero, R., J. A. Guijarro, C. Ramis, and S. Alonso (1998), A 30 year (1964–1993) daily rainfall data base for the Spanish Mediterranean regions: First exploratory study, *Int. J. Climatol.*, *18*, 541–560.

Romero, R., G. Summer, C. Ramis, and A. Genovés (1999a), A classification of the atmospheric circulation patterns producing significant daily rainfall in the Spanish Mediterranean area, *Int. J. Climatol.*, *19*, 765–785.

Romero, R., C. Ramis, and J. A. Guijarro (1999b), Daily rainfall patterns in the Spanish Mediterranean area: An objective classification, *Int. J. Climatol.*, *19*, 95–112.

Serra, T., J. Colomer, L. Zamora, R. Moreno-Amich, and X. Casamitjana (2002), Seasonal development of a turbid hydrothermal plume in a lake, *Water Res.*, *36*, 2753–2760.

Serra, T., J. Colomer, R. Julià, M. Soler, and X. Casamitjana (2005), Behaviour and dynamics of a hydrothermal plume in Lake Banyoles, Catalonia, *Sedimentology*, *52*, 795–805.

Summer, G., J. A. Guijarro, and C. Ramis (1995), The impact of surface circulations on the daily rainfall over Mallorca, *Int. J. Climatol.*, *15*, 673–696.

Summer, G. N., R. Romero, V. Homar, C. Ramis, S. Alonso, and E. Zorita (2003), An estimate of the effects of climate change on the rainfall of Mediterranean Spain by the late twenty first century, *Clim. Dyn.*, *20*, 789–805.

Weyhenmeyer, G. A., T. Blenckner, and K. Pettersson (1999), Changes of the plankton spring outburst related to the North Atlantic Oscillation, *Limnol. Oceanogr.*, *44*, 1788–1792.

Yarnal, B. (1993), *Synoptic Climatology in Environmental Analysis*, Belhaven, London.

J. Colomer, T. Serra, and M. Soler, Group of Environmental Physics, Physics Department, University of Girona, Campus Montilivi, E-17071 Girona, Spain. (marianna.soler@udg.es)

R. Romero, Meteorology Group, Physics Department, University of the Balearic Islands, E-07122 Palma de Mallorca, Spain.